End Pressure Corrections in Capillary Rheometry of Concentrated Suspensions

Z. Y. Wang,[1] S. C. Joshi,[2] Y. C. Lam,[1,3] X. Chen[3]

[1]*Division of Manufacturing Engineering, School of Mechanical and Aerospace Engineering, Nanyang Technological University, Singapore 639798*
[2]*Division of Aerospace Engineering, School of Mechanical and Aerospace Engineering, Nanyang Technological University, Singapore 639798*
[3]*Singapore-MIT Alliance Programme, Nanyang Technological University, Singapore 639798*

Received 2 April 2008; accepted 22 March 2009
DOI 10.1002/app.30444
Published online 24 June 2009 in Wiley InterScience (www.interscience.wiley.com).

ABSTRACT: The end effect of a capillary die was investigated on concentrated suspensions with different particle concentrations, using dies with different diameters and at different temperatures. Nonlinearity in the Bagley plots was observed experimentally, and the nonlinearity increased with increasing particle concentration, decreasing temperature, and smaller capillary dies. Calculated end pressures based on the nonlinear Bagley plots were compared with those measured using an orifice die. As the extruded melts tended to stick on the exit wall of the capillary die, measurements by orifice die registered (40–50%) higher losses than those obtained from Bagley corrections. The key factors, which include particle concentration, contraction ratio, temperature, and flow rate, were discussed for their effects on end pressure. A formula was proposed combining the effects of these factors. Good agreement was obtained between the calculated end pressures with predicted results by the proposed formula. © 2009 Wiley Periodicals, Inc. J Appl Polym Sci 114: 1738–1745, 2009

Key words: end pressure; Bagley correction; concentrated suspension

INTRODUCTION

In capillary rheometry, there is a large pressure drop associated with the flow in the entrance and exit regions. These two pressure losses are collectively known as the end pressure,[1] ΔP_e. Its determination is important for the proper evaluation of the true wall shear stress and shear viscosity. ΔP_e has also been used for estimation of extensional viscosity.[2–4] Zirnsak et al.[5] gave a good review of the theories related to suspension, and their ability to predict the steady shear and extensional viscosities, as well as the first normal stresses observed in dilute and semiconcentrated solutions.

Entrance loss plays a major role in the end pressure. Thus, some researchers ignored the effect of exit loss and assumed that the total pressure loss to be the entrance loss.[6,7] However, the total pressure loss determined (either by Bagley correction or measured directly by orifice die) should be considered as the sum of entrance and exit losses.[8,9] Entrance loss is dependent on the ratio of capillary diameter to barrel diameter (D/D_{barrel}) and decreases with increasing ratio. If the ratio reaches unity, there is no entrance loss.

Correspondence to: Y. C. Lam (myclam@ntu.edu.sg).

Journal of Applied Polymer Science, Vol. 114, 1738–1745 (2009)

A Bagley plot is a graph showing capillary pressure drop versus the die length to radius (L/R) ratio, with apparent wall shear rate as a parameter. The end pressure is obtained by extrapolating to $L/R = 0$. For Newtonian fluids at low Reynolds numbers, exit loss should be zero and the entrance loss should be very small. Thus, the end pressure drop is thought to reflect the elasticity of the melt.[10] However, for non-Newtonian polymeric melts, the interpretation of the end pressure is complicated by the dependence of viscosity on pressure, viscous heating, and/or wall slip. If all these factors are negligible, the Bagley plot is expected to be linear. If the viscosity is dependent on pressure, the Bagley plot exhibits an upward curvature.[11] The deviation from linearity in the Bagley plot could have its origin in viscous heating and/or wall slip. Wall slip reduces the shear rate. With slip velocity decreases with hydraulic pressure, the shear rate will depend on the axial position in the channel. This will result in a concave Bagley plot.[12]

For a concentrated suspension with particles dispersed in a polymeric melt, particle migration is a potentially important parameter to be considered but hitherto received little attention. The nonuniform velocity gradient, and thus shear rate, in a capillary flow results in particles migrating from regions of high shear to regions of low shear.[8,13,14] Thus a homogeneous suspension becomes inhomogeneous as it flows down the capillary, with particle migrating away from

the wall to the center of the capillary. The effect of particle migration increases with increasing ratio of die length to die radius, resulting in a convex Bagley plot.

Orifice die is an alternative to Bagley correction for the determination of ΔP_e. With minimum die length, it has the potential to avoid errors due to the pressure dependency of viscosity, viscous heating, and wall slip. The important parameters of an orifice die for the measurement of ΔP_e include the L/R of the orifice, the entrance angle, and the contraction ratio (barrel diameter over orifice diameter). Kelly et al.[15] found that if the land, L, is not longer than 0.5 mm, it has little effect on the experimental result.

However, there have been reports of discrepancies between the end pressure determined by an orifice die and by Bagley plot. Padmanabhan[16] found that ΔP_e from Bagley plots are higher than those measured using an orifice die for the material IUPAC-X. In contrast, Rides et al.[17] reported that ΔP_e measured by an orifice die was about 10% higher than those determined by Bagley plot for the polymer HDPE.

The diameter in the orifice exit section is an important parameter as it affects the flow of the extruded melt.[7] If the melt is stuck in the expansion region, it would result in a higher measured ΔP_e than what should be the true value.

While it is clear that the end pressure is related to many parameters, there are few in-depth studies on their effects, and their mutual interactions. A notable exception is the work by Jastrzebski,[6] who proposed a formula correlating end pressure with flow rate and die diameter. However, the effect of temperature has not been considered, and there is a lack of experimental verification. These will be the focus of this investigation.

EXPERIMENTAL

Materials

The model materials employed are pure polymer ethylene vinyl acetate 460 (EVA460), with density of 941 kg/m^3, and concentrated suspensions consisting of EVA460 mixed with spherical glass microspheres with sizes ranging from 53 to 63 μm. The density of glass beads is 2500 kg/m^3. Polymer EVA460 was manufactured by Dupont (USA) under the trade name ELVAX. EVA is a copolymer of ethylene and vinyl acetate (VA); EVA460 contains 18% VA by weight with melt index of 2.5 and melting point of 88°C. Glass powder is manufactured by MO-SCI Corp. (USA). The soda-lime glass contains more than 60% silicon, with a minimum of 90% true spheres in the specified size range.

Equipment

A capillary rheometer (Göttfert Capillary Rheograph 6000) with a continuously variable piston speed was used in this work. A standard barrel with diameter of 12 mm and a length of 200 mm was employed. Capillary dies with diameter of 0.5, 1, and 2 mm were used in the Bagley correction, with the ratio (L/D) ranging from 5 to 80. An orifice die with diameter of 1 mm and die length of 0.5 mm was also employed (Fig. 1).

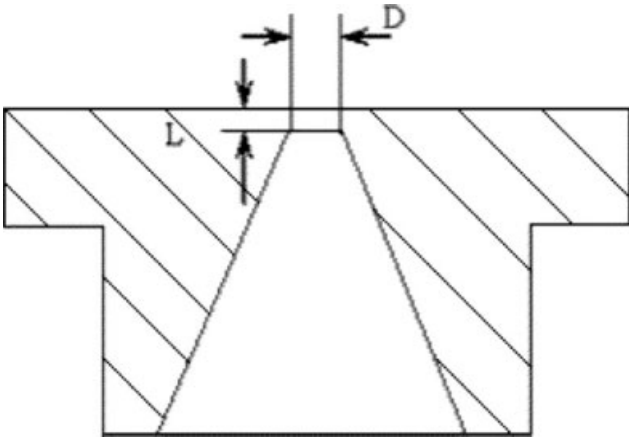

Figure 1 Sketch of a capillary orifice die.

RESULTS AND DISCUSSIONS

In the characterization of the flow behavior of concentrated suspension by capillary rheometry, the important factors, which include buoyancy effect, pressure-dependent viscosity, viscous heating, particle migration, and wall slip, should be discussed as they may be dominant in some cases and thus affect the measured pressure.

Buoyancy effect

In addition to the diffusive effect of particles, buoyancy forces could also affect particle migration when the particle density differs significantly from that of the suspending fluid. The effect of buoyant forces can be evaluated by the buoyant number as follows[18]:

$$N_B = \frac{2(\rho_p - \rho_b)gR^2}{9\eta U} \quad (1)$$

where ρ_p is the density of the particles, ρ_b is the density of the fluid, e.g., a polymer melt, g is the acceleration due to gravity, R is the radius of the pipe, η is the viscosity, and U is the average axial velocity.

Carpen and Brady[19] found that as the density difference between the particles and the suspending fluid increases, instability becomes more pronounced.

However, the effect of buoyancy of particles on particle flux can be neglected in this study because of the high viscosity of EVA employed and the small difference of density between the polymer matrix

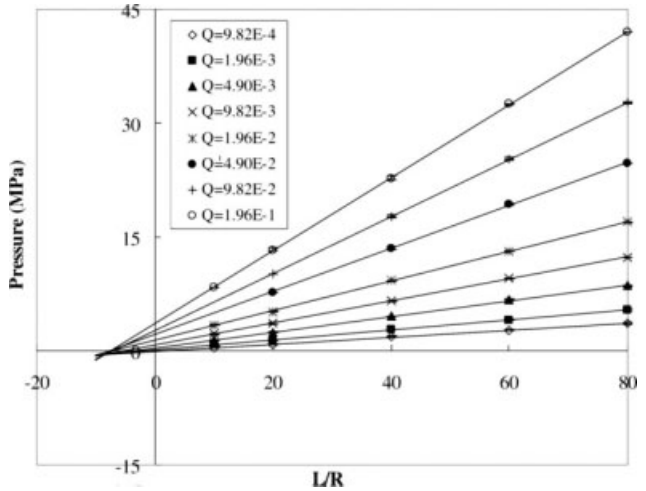

Figure 2 Bagley plot of pure EVA460 at 180°C for 1 mm die diameter (Q, cm^3/s).

and the glass particles in the investigation, where the buoyant number N_B is less than 0.01.[20]

Pressure-dependent viscosity

Pressure-dependent viscosity can be determined either from the nonlinearity in a Bagley plot or from the pressure profile generated during flow in a slit geometry.[21–24]

Figure 2 shows the Bagley plot of pure EVA460 at 180°C. The experiments were repeated three times at the same conditions. The error bars indicate that the repeatability of the measurements was good, with less than 4% difference between the experiments at the same conditions. A good repeatability of EVA-silica suspensions at different conditions implied that it is a stable system.

The curves in this figure show good linearity, indicating pressure-dependent viscosity negligible. Compared with the case of pure binder, the effect of pressure-dependent viscosity should be lower for concentrated suspension as rigid particles suspended

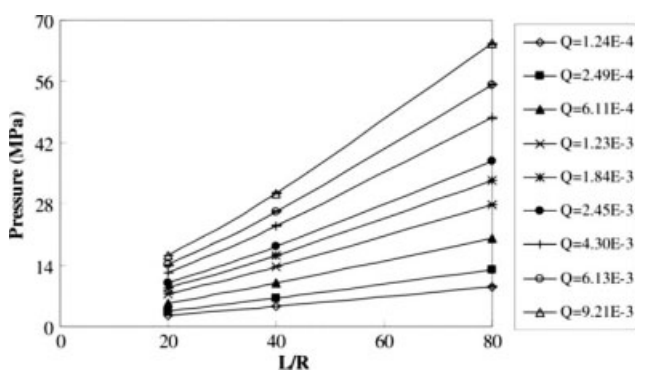

Figure 3 Bagley plot for concentrated suspension with $\phi = 40\%$ for 0.5 mm die diameter at 180°C (Q, cm^3/s).

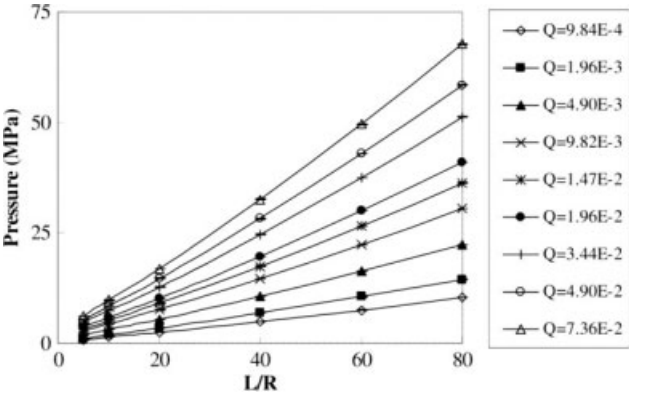

Figure 4 Bagley plot for concentrated suspension with $\phi = 40\%$ for 1 mm die diameter at 180°C (Q, cm^3/s).

in the polymer system reduce the compressibility.[20] Therefore, the nonlinearity in the Bagley plot of concentrated suspension can only be attributed to other effects.

Nonlinear Bagley plot

As the effects of buoyancy effect and pressure-dependent viscosity are negligible, the flow of concentrated suspension in this investigation will be mainly controlled by particle migration, wall slip, and viscous heating. The effect of viscous heating is related to shear rate. In this study, the shear rate was set in a relatively low range of 0–750 s^{-1}, where the viscous heating effect can be ignored,[20] and thus the fluid can be regarded to be in an isothermal condition.

Therefore, particle migration and wall slip are two important issues remaining in our study of the suspension rheology. Both of them affect pressure, but in a different way. As presented in our previous work,[20] a Bagley plot will become convex with particle migration, and in contrast, it will become concave with wall slip.

Figures 3–5 show examples of Bagley plots for suspensions with the same particle concentration of

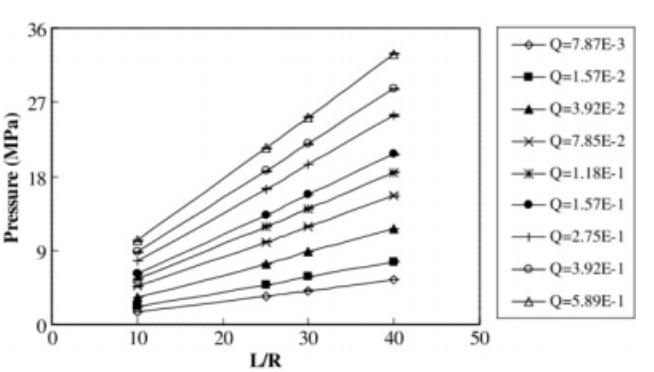

Figure 5 Bagley plot for concentrated suspension with $\phi = 40\%$ for 2 mm die diameter at 180°C (Q, cm^3/s).

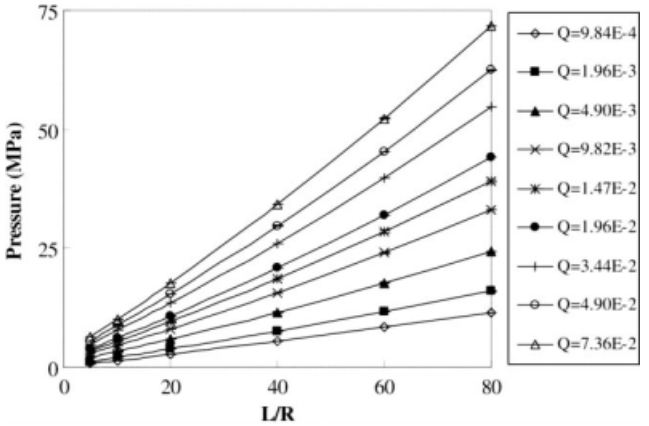

Figure 6 Bagley plot for concentrated suspension with $\phi = 45\%$ for 1 mm die diameter at 180°C (Q, cm^3/s).

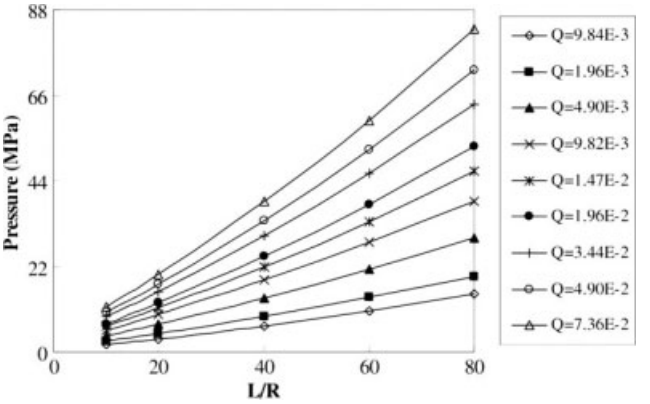

Figure 7 Bagley plot for concentrated suspension with $\phi = 40\%$ for 1 mm die diameter at 160°C (Q, cm^3/s).

40% by volume, but for different die diameters at 180°C. All experiments were conducted at least three times. The repeatability of the data was indicated by the small error bars in the figures. The nonlinearity in the Bagley plot increases with decreasing capillary diameter and also with flow rate significantly.

In addition to die diameter, the curves in the Bagley plot are also affected by particle concentration and temperature. Figures 4 and 6 show the effect of particle concentrations of 40 and 45%, respectively. Figures 4 and 7 show the effect of temperature at 180 and 160°C, respectively. The results in these figures indicate that the nonlinearity of the curves increases with increasing particle concentration and/or with decreasing temperature.

The shear-induced particle migration is greater for smaller capillaries, higher shear rate, and higher particle concentration. However, it also causes larger slip along the wall because of the formation of a thin, dilute layer near the wall with low viscosity. The concave nonlinearity in the Bagley plots implied that the effect of wall slip is larger than that of particle migration.

Determination of end pressure

For pure EVA460, linear prediction can be employed to estimate the end pressure. However, for concentrated suspension, the end pressures would not be predicted well using linear prediction because of the nonlinearity in the Bagley plots (other than 2 mm diameter die). Instead, the end pressure can be determined by correcting for pressure associated with the end effects in a Bagley plot using a second order polynomial[8]:

$$\Delta P = a(L/R)^2 + b(L/R) + \Delta P_e \quad (2)$$

where ΔP is the total measured pressure, a and b are constants related to the flow rate, particle concentration, and temperature; ΔP_e is the end pressure.

ΔP_e, a, and b in eq. (2) can be determined by polynomial curve fitting. Table I lists the fitting results at the same temperature but with different particle concentrations. It is observed that with increasing particle concentration, both the constants and the end pressure increase. Table II shows the results of end pressures with the same particle concentration of

TABLE I
Fitted Results of End Pressure at 180°C with Different Particle Concentrations for 1 mm Die Diameter

	Fitted results at same temperature								
	35%			40%			45%		
Q (cm^3/s)	a (MPa)	b (MPa)	ΔP_e (MPa)	a (MPa)	b (MPa)	ΔP_e (MPa)	a (MPa)	b (MPa)	ΔP_e (MPa)
9.84 E-04	0.0002	0.01	0.31	0.0002	0.11	0.36	0.0002	0.13	0.38
1.96 E-03	0.0003	0.13	0.48	0.0003	0.15	0.51	0.00032	0.17	0.54
4.90 E-03	0.0006	0.20	0.79	0.0006	0.23	0.82	0.00064	0.24	0.86
9.82 E-03	0.0007	0.28	1.12	0.0008	0.31	1.16	0.00093	0.33	1.20
1.47 E-02	0.0008	0.34	1.38	0.0009	0.37	1.40	0.0011	0.38	1.46
1.96 E-02	0.0009	0.38	1.56	0.001	0.41	1.61	0.00125	0.43	1.68
3.44 E-02	0.0011	0.47	2.03	0.0012	0.52	2.06	0.0015	0.53	2.24
4.90 E-02	0.013	0.53	2.40	0.0014	0.59	2.50	0.0017	0.61	2.61
7.36 E-02	0.0015	0.63	2.88	0.0017	0.68	3.02	0.0019	0.71	3.17

TABLE II
Fitted End Pressures at Different Temperatures for Concentrated Suspension of ϕ = 40% for 1 mm Die Diameter

	Fitted end pressure results at same particle concentration								
	$T = 210°C$			$T = 180°C$			$T = 160°C$		
Q (cm^3/s)	a (MPa)	b (MPa)	ΔP_e (MPa)	a (MPa)	b (MPa)	ΔP_e (MPa)	a (MPa)	b (MPa)	ΔP_e (MPa)
9.84 E-04	0.00009	0.07	0.08	0.0002	0.11	0.36	0.0003	0.13	0.64
1.96 E-03	0.0001	0.11	0.17	0.0003	0.15	0.51	0.0005	0.17	0.81
4.90 E-03	0.0004	0.15	0.47	0.0006	0.23	0.82	0.0007	0.28	1.30
9.82 E-03	0.0005	0.22	0.70	0.0008	0.31	1.16	0.0009	0.38	1.68
1.47 E-02	0.0007	0.26	0.91	0.0009	0.37	1.40	0.0011	0.43	2.11
1.96 E-02	0.0008	0.28	1.14	0.001	0.41	1.61	0.0012	0.48	2.36
3.44 E-02	0.001	0.37	1.53	0.0012	0.52	2.06	0.0014	0.59	2.87
4.90 E-02	0.0012	0.43	1.90	0.0014	0.59	2.50	0.0016	0.66	3.28
7.36 E-02	0.0014	0.51	2.26	0.0017	0.68	3.02	0.002	0.76	3.75

40% but at different temperatures. The constants a and b and the end pressure ΔP_e increase with decreasing temperature. The standard deviations between the predicted pressures with experimental data are less than 0.08 MPa, showing good agreement between them.

Formula of end pressure

By curve fitting, end pressures were obtained for various flow rates, capillary radii, particle concentrations, and temperatures. However, a proper expression to correlate their relationship is yet to be developed. In 1967, Jastrzebski proposed a power-law function to correlate ΔP_e with the volumetric flow rate, Q, as follows:

$$\Delta P_e = Be^{cR}Q^n \tag{3}$$

where B is a characteristic constant for a given concentration, c is a constant related to die radius R, and n is the flow index.

However, Jastrzebski[6] did not consider the effect of temperature. Experimental results showed that temperature affects the constant n. The higher the temperature, the larger the constant n, and thus the lower the end pressure. The parameter B is found to be dependent on particle concentration. In addition, the end pressure relates directly to the contraction ratio of capillary diameter to barrel diameter, which is not well reflected by eq. (3). Therefore, the expression for end pressure is modified to

$$\Delta P_e = f(\phi)f(D/D_{\text{barrel}})Q^{f(T)} \tag{4}$$

where ϕ, D, and T are particle concentration, die diameter, and temperature, respectively. In our experiment, $D_{\text{barrel}} = 12$ mm.

The functions of $f(\phi)$, $f(D/D_{\text{barrel}})$, $f(T)$ in eq. (4) can be obtained from experimental data in the following sequence:

1. For a given particle concentration and die diameter, plot $\log(\Delta P_e)$ versus $\log(Q)$ at different temperatures (Fig. 8). It shows that $\log(\Delta P_e)$ is linear to $\log(Q)$ at high flow rates, but data points deviated from linearity at very low flow rates. This is due to the reason that any small experimental error in pressure measurement can result in significant percentage error because of the small pressure registered at low flow rate. Therefore, the deviation from the linearity at very low flow rates can be neglected, and from the slopes of the curves in Figure 8, $f(T)$ can be determined.
2. At a given temperature, the plot of $\log(\Delta P_e/Q^{f(T)})$ versus $\log(D/D_{\text{barrel}})$ for a given particle concentration is shown in Figure 9, showing a linear relationship between them. Therefore, $f(D/D_{\text{barrel}})$ can be expressed as follows:

$$f(D/D_{\text{barrel}}) = \left(\frac{D}{D_{\text{barrel}}}\right)^k \tag{5}$$

where the constant k can be obtained by the slope in Figure 9.

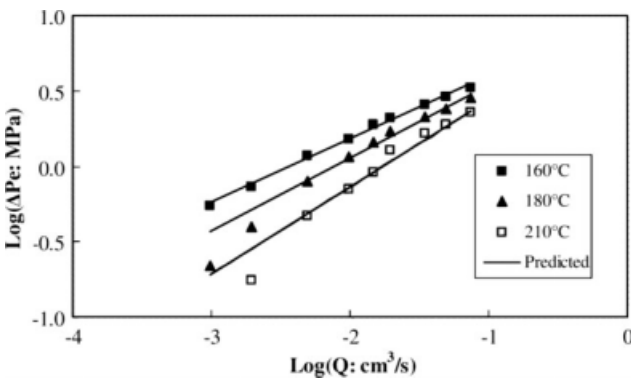

Figure 8 $\log(\Delta P_e)$ versus $\log(Q)$ for concentrated suspensions with $\phi = 40\%$ at different temperatures for 1 mm die diameter.

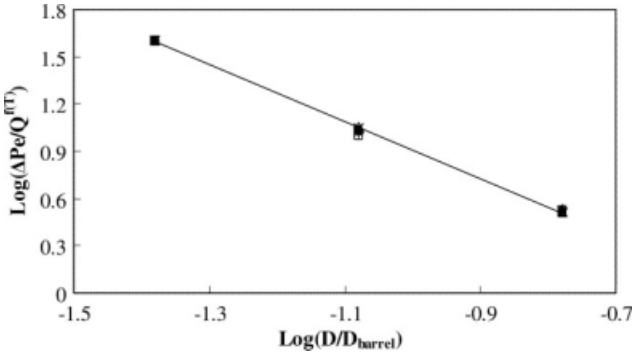

Figure 9 $\log(\Delta P_e/Q^{f(T)})$ versus $\log(D/D_{\text{barrel}})$ for concentrated suspension with $\phi = 40\%$ at 180°C for different dies.

3. For a given die diameter and temperature, plot $f(\phi) = \frac{\Delta P_e}{(D/D_b)^k Q^{f(T)}}$ versus ϕ for suspensions with different particle concentrations (Fig. 10). $f(\phi)$, which is a linear function of ϕ, can be determined from the fitted line.

Particle concentration affects the end pressure, but its effect is not as significant as the contraction ratio and temperature. This is because with a relatively small increase in particle concentration, the flow profile at the contraction will remain similar, and thus the pressure loss will not differ significantly. In contrast, the contraction ratio has a significant effect on the flow profile, and the temperature affects the overall viscosity. Thus, these two parameters can be expected to have much more significant effects on end pressure than particle concentration.

From these experimental investigations, eq. (4) can be rewritten as follows:

$$\Delta P_e = c_1(\phi + c_2)\left(\frac{D}{D_{\text{barrel}}}\right)^k Q^{m_1 T + m_2} \tag{6}$$

where c_1, c_2, m_1, and m_2 are material constants. The fitted parameters for the system investigated are listed in Table III. These fitted values were specific to the investigated system and should be different for different fillers because of different surface interaction between particles and polymer matrix. However, the same methodology can be extended to these systems.

TABLE III
Fitted Parameters in Eq. (6)

$f(\phi)$	c_1	0.1
	c_2	0.7
$f(D/D_{\text{barrel}})$	k	−1.84
$f(T)$	m_1 (1/K)	4×10^{-3}
	m_2	−1.32

When $D = D_{\text{barrel}}$, there is no entrance loss and eq. (6) should predict exit loss only.

End pressure by orifice die

End pressure can also be estimated directly using an orifice die. Figure 11 shows a comparison of the end pressures measured by orifice die and nonlinear Bagley correction, with the data obtained by orifice die higher by 40–50%. Careful examination of our experiments indicated that the extruded melt had a tendency to stick to the exit wall, with insufficient time for the extruded melt to cool down before it touched the wall of the design, as shown in Figure 1. This is consistent with the finding of Kim and Dealy,[7] in which the exit shape of an orifice die is important as it affects the flow of the extruded melt. If the melt is stuck in the expansion region, it will result in higher flow resistance, and thus a higher end pressure measured than what it should be.

Discussions

The end pressures calculated by Bagley correction were compared with the predicted values by eq. (6)

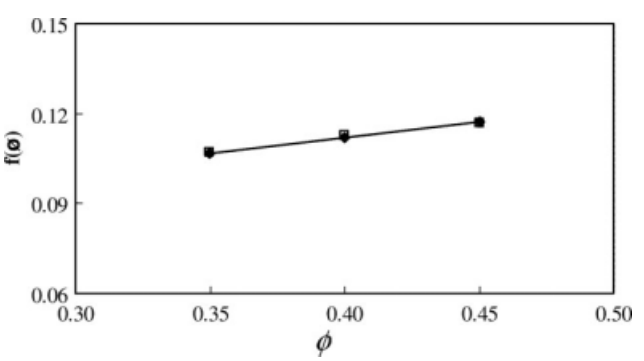

Figure 10 $f(\phi)$ versus ϕ for suspensions with different particle concentrations at 180°C for 1 mm die diameter.

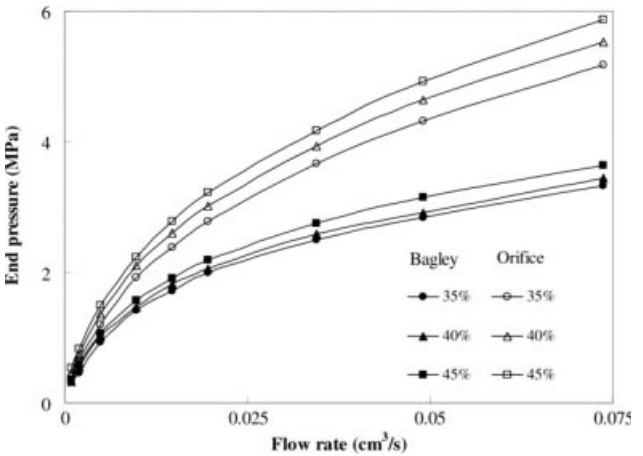

Figure 11 Comparison of end pressures by orifice die and nonlinear Bagley plot for suspensions with different particle concentrations at 180°C for 1 mm die diameter.

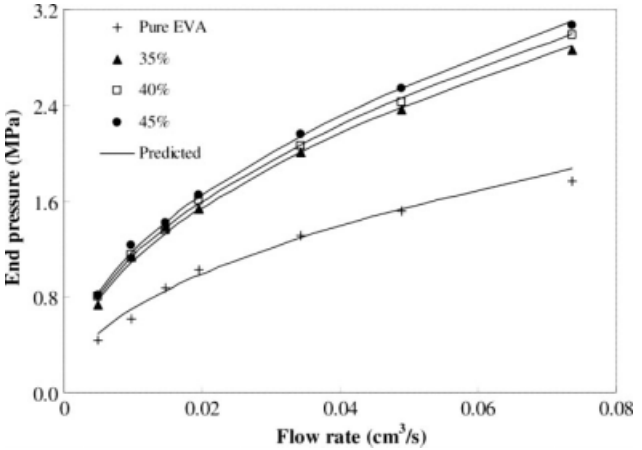

Figure 12 Comparison of end pressures by Bagley correction and predicted results by eq. (6) for pure EVA 460 and suspensions with different particle concentrations for 1 mm die diameter at 180°C.

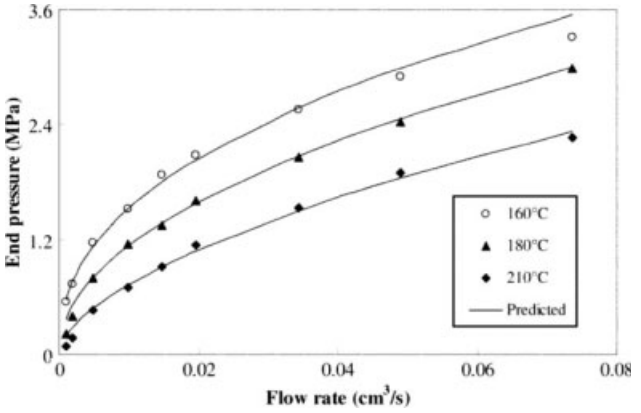

Figure 14 Comparison of end pressures by Bagley correction and predicted results by eq. (6) at different temperatures for concentrated suspension with $\phi = 40\%$ for 1 mm die diameter.

for both pure binder and concentrated suspensions (Figs. 12–14). For pure polymer melts, the end pressure can be predicted by setting $\phi = 0$.

Figure 12 shows the end pressures with different particle concentrations ($\phi = 0$, 35%, 40%, 45%). Good agreement was obtained between Bagley correction and eq. (6).

Figure 13 shows the good agreement obtained for end pressure between nonlinear Bagley correction and eq. (6) for different contraction ratios ($D/D_{\text{barrel}} = 1/24, 1/12, 1/6$), for a suspension with 40% particle concentration at 180°C. This agrees with the suggestion of Rides and Allen[25] that end pressure is a function of the contraction ratio. With small dies (i.e., higher ratio of barrel diameter to capillary diameter), ΔP_e is higher and is sensitive to flow rate.

Figure 14 shows good agreement obtained for the effect of temperature on end pressure between nonlinear Bagley correction and eq. (6) for a suspension with 40% particle concentration and die diameter of 1 mm.

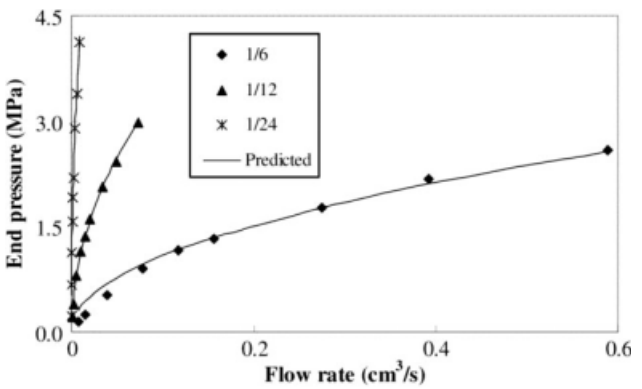

Figure 13 Comparison of end pressures by Bagley correction and predicted results by eq. (6) at different contraction ratios (D/D_{barrel}) for concentrated suspension with $\phi = 40\%$ at 180°C.

CONCLUSIONS

Our investigation indicated that for concentrated suspension, end pressures should be obtained with nonlinear Bagley corrections as the nonlinearity in the Bagley plot could be significant. End pressure obtained by orifice die could be higher than the actual values because of the sticking of the polymer on the exit die wall. The expression developed in this investigation correlating the combined effects of particle concentration, contraction ratio, and temperature could predict well the end pressure.

References

1. Mitsoulis, E.; Hatzikiriakos, S. G. Rheol Acta 2003, 42, 309.
2. Gibson, A. G. In Convering Dies in Rheological Measurements; Collyer, A. A., Clegg, D. W., Eds.; Chapman and Hall: London, 1998; Chapter 15.
3. Gotsis, A. D.; Odriozola, A. Rheol Acta 1998, 37, 430.
4. Mitsoulis, E.; Hatzikiriakos, S. G.; Christodoulou, K.; Vlassopoulos, D. Rheol Acta 1998, 37, 438.
5. Zirnsak, M. A.; Hur, D. U.; Boger, D. V. J Non-Newtonian Fluid Mech 1994, 54, 153.
6. Jastrzebski, Z. D. Ind Eng Chem Fundam 1967, 6, 445.
7. Kim, S.; Dealy, J. M. J Rheol 2001, 45, 1413.
8. Macosko, C. M. Rheology, Principles, Measurements and Applications; VCH Publishers: New York, 1994.
9. Laun, H. M. Rheol Acta 2003, 42, 295.
10. Dealy, J. M.; Wissbrun, K. F. Melt Rheology and Its Role in Plastics Processing; VNR Publisher: New York, 1995.
11. Laun, H. M.; Schuch, H. J Rheol 1989, 33, 119.
12. Hatzikiriakos, S. G.; Dealy, J. M. J Rheol 1992, 36, 703.
13. Leighton, D.; Acrivos, A. J Fluid Mech 1987, 181, 415.
14. Lam, Y. C.; Chen, X.; Tan, K. W.; Chai, J. C.; Yu, S. C. M. Compos Sci Technol 2004, 64, 1001.

15. Kelly, A. L.; Coates, P. D.; Dobbie, T. W.; Fleming, D. J Plast Rub Comp Proc Appl 1996, 25, 313.
16. Padmanabhan, M. Evaluation of the Entrance Pressure Drop Method to Estimate Extensional Viscosity, Masters Thesis; University of Minnesota: Minnesota, 1993.
17. Rides, M.; Allen, C. R. G.; Chakravorty, S. National Physics Laboratory Report CMMT(A) 171, 1999.
18. Norman, J. T.; Nayak, H. V.; Bonnecaze, R. T. J Fluid Mech 2005, 523, 1.
19. Carpen, I. C.; Brady, J. F. J Fluid Mech 2002, 472, 201.
20. Wang, Z. Y.; Lam, Y. C.; Joshi, S. C.; Chen, X. Polym Compos, to appear.
21. Hatzikiriakos, S. G.; Dealy, J. M. Polym Eng Sci 1994, 34, 493.
22. Moldenaers, P.; Vermant, J.; Mewis, J.; Heynderickx, I. J Rheol 1996, 40, 203.
23. Hay, G.; Mackay, M. E.; Awati, K. M.; Park, Y. J Rheol 1999, 43, 1099.
24. Liang, J. Z. Polymer 2001, 42, 3709.
25. Rides, M.; Allen, C. R. G. National Physics Laboratory Report CMMT(A) 25, 1996.